PROTEINS: Structure, Function, and Genetics 35:275–282 (1999)

CRITICAL REVIEW

High-Precision Measurement of Hydrogen Bond Lengths in Proteins by Nuclear Magnetic Resonance Methods

Thomas K. Harris and Albert S. Mildvan*
Department of Biological Chemistry, The Johns Hopkins University School of Medicine, Baltimore, Maryland

ABSTRACT **We have compared hydrogen bond lengths on enzymes derived with high precision (≤ ±0.05 Å) from both the proton chemical shifts (δ) and the fractionation factors (ϕ) of the proton involved with those obtained from protein X-ray crystallography. Hydrogen bond distances derived from proton chemical shifts were obtained from a correlation of 59 O—H···O hydrogen bond lengths, measured by small molecule high-resolution X-ray crystallography, with chemical shifts determined by solid-state nuclear magnetic resonance (NMR) in the same crystals (McDermott A, Ridenour CF, Encyclopedia of NMR, Sussex, U.K.: Wiley, 1996:3820–3825). Hydrogen bond distances were independently obtained from fractionation factors that yield distances between the two proton wells in quartic double minimum potential functions (Kreevoy MM, Liang TM, J Am Chem Soc, 1980;102:3315–3322). The high-precision hydrogen bond distances derived from their corresponding NMR-measured proton chemical shifts and fractionation factors agree well with each other and with those reported in protein X-ray structures within the larger errors (±0.2–0.8 Å) in distances obtained by protein X-ray crystallography. The increased precision in measurements of hydrogen bond lengths by NMR has provided insight into the contributions of short, strong hydrogen bonds to catalysis for several enzymatic reactions. Proteins 1999;35:275–282.** © 1999 Wiley-Liss, Inc.

Key words: chemical shift; fractionation factor; triosephosphate isomerase, ketosteroid isomerase; chymotrypsin; chymotrypsinogen; subtilisin; serine protease

INTRODUCTION

Major contributions to catalysis by many enzymes are provided by hydrogen bonds from catalytic groups of the enzyme to sites on the bound substrate or between enzymatic residues themselves. The participation of multiple hydrogen bonds at the enzyme active site can result in transition-state stabilization and thereby account for a significant amount of the rate enhancement observed for many enzymes.[1] The roles of specific hydrogen bonds in catalysis have most often been inferred from X-ray or NMR structures of enzymes and enzyme–ligand complexes. However, the resolution of most protein structures precludes an exact or precise measurement of hydrogen bond distances. The distances obtained by protein X-ray diffraction, as a rule of thumb, have errors ranging from 0.1 to 0.3 times the resolution, depending on the local quality of the data. Hence a 2.0–Å resolution X-ray structure of an enzyme can measure hydrogen bond distances to within ±0.2 to ±0.6 Å.[2] Because hydrogen bond distance changes in the range ±0.1 Å result in significant changes in the strength of the hydrogen bond,[3] a more accurate and precise method for measuring hydrogen bond distances would be of great value.

Hydrogen bonds in nature range in strength from very weak ($\Delta G_{formation} \approx -2$ kcal/mol) to very strong ($\Delta G_{formation} < -25$ kcal/mol) depending on the hydrogen bond distance.[3] In weak hydrogen bonds, the proton is covalently bonded to one electronegative atom at a distance of ≈1.0 Å, and electrostatically attracted to another electronegative atom at approximately twice the distance (1.7–2.0 Å) (Fig. 1A). The overall hydrogen bond length, given by the distance between the two electronegative or heavy atoms is 2.7–3.0 Å. The proton has two alternative locations or free energy wells because it can be covalently bonded either to A or to B [Eq. (1)].

$$\begin{array}{c} \text{—A—H----:B—} \\ \Updownarrow \\ \text{—A:---- H—B—} \end{array} \qquad (1)$$

Abbreviations: LBHB, low-barrier hydrogen bond; SSHB, short, strong hydrogen bond; NMR, nuclear magnetic resonance; TIM, triosephosphate isomerase; PGH, phosphoglycolohydroxamic acid; DHAP, dihydroxyacetone phosphate; GAP, glyceraldehyde 3-phosphate; KSI, ketosteroid isomerase; DHE, dihydroequilenin; BoroPhe, methoxysuccinyl-Ala-Ala-Pro-2-amino-3-phenylethylboronic acid; *N*-AcF-CF_3, *N*-acetyl-L-phenylalanyl-trifluoromethyl ketone; *N*-AcLF-CF_3, *N*-acetyl-L-leucyl-L-phenylalanyl-trifluoromethyl ketone; sAAPF, succinyl-alanyl-alanyl-prolyl-phenylalanine.

Grant sponsor: National Institutes of Health; Grant number: DK 28616.

*Correspondence to: Albert S. Mildvan, Department of Biological Chemistry, The Johns Hopkins School of Medicine, 725 North Wolfe Street, Baltimore, MD 21205. E-mail: mildvan@welchlink.welch.jhu.edu

Received 17 November 1998; Accepted 21 January 1999

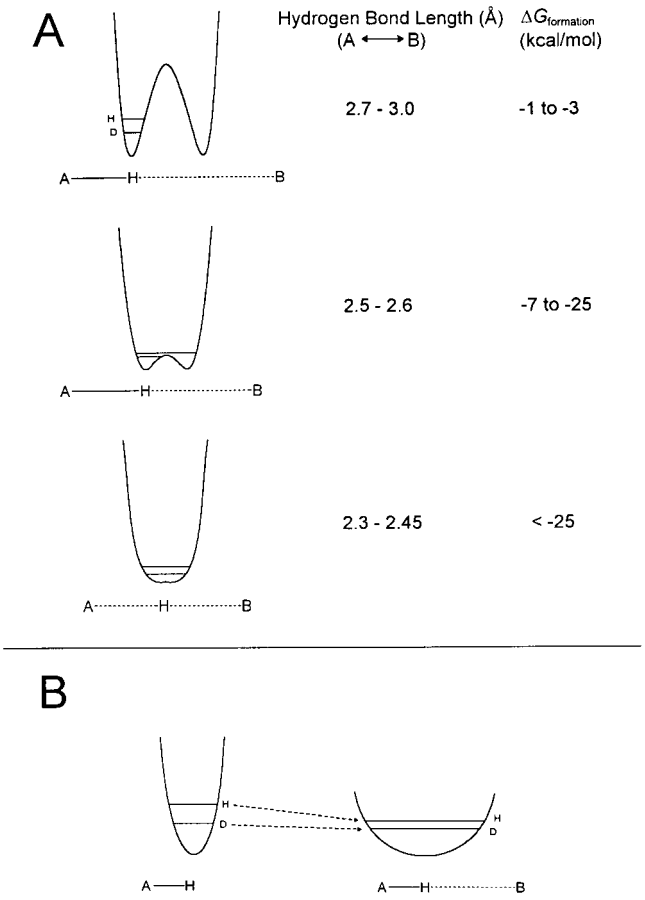

Fig. 1. **(A)** Potential functions for weak, double-well (*upper*), strong, low-barrier (*middle*), and very strong, single-well hydrogen bonds (*lower*) in which the pK_a values of A—H and B—H are equal. The horizontal lines give the zero-point vibrational energy levels of protium and deuterium. Also shown are the lengths and strengths of such hydrogen bonds. **(B)** Effect of hydrogen bonding on the effective force constant and resulting zero-point vibrational energies of a proton and a deuteron.

As the electronegative atoms A and B approach each other, shortening the hydrogen bond to values between 2.70 and 2.50 Å, the covalent A—H moiety lengthens, the noncovalent moiety H···B shortens, the hydrogen bond becomes stronger (-7 kcal/mol $\geq \Delta G_{\text{formation}} \geq -25$ kcal/mol) and the barrier between the two proton wells becomes lower (Fig. 1A).[3–5] The state often referred to as an LBHB occurs when the barrier height approaches the zero point vibrational energy of hydrogen, and the proton becomes delocalized between the two wells while a deuteron would remain localized (Fig. 1A). Specifically, as O—H···O hydrogen bond lengths decrease from 2.54 Å to 2.45 Å, their strengths ($\Delta E_{\text{formation}}$) increase rapidly from -7.8 kcal/mol to -32 kcal/mol,[3] presumably due to exponentially increasing overlap of the proton and oxygen wavefunctions. As the heavy atoms continue to approach each other, further shortening the hydrogen bond lengths to values between 2.45 and 2.30 Å, the barrier between the wells disappears and the proton (or deuteron) is in a single well (Fig. 1A). In such single-well hydrogen bonds, which are very strong ($\Delta G_{\text{formation}} < -25$ kcal/mol), the average position of the proton is now equidistant from the two electronegative atoms. Single-well hydrogen bonds have not been reported in proteins. While the strength of hydrogen bonds correlates strongly with their lengths (Fig. 1A), little or no correlation of strength with hydrogen bond angle, over a range of 180 ± 30° is found experimentally[6] or theoretically.[7] Angle bending beyond ±30° can lead to weakening of strong hydrogen bonds.[8]

In aqueous environments, due to competition with the solvent, weak hydrogen bonding is expected and is generally found.[9] Thus the average strength of hydrogen bonds contributing to protein structure has been estimated calorimetrically as $\Delta G_{\text{formation}} \approx -2 \pm 1$ kcal/mol.[10] Similarly, in nucleic acids the hydrogen bonds responsible for base pairing are comparably weak.[11] However, several examples in biological systems have been reported in which hydrogen bonds are shorter and stronger than average with $\Delta G_{\text{formation}} \leq -7$ kcal/mol and with lengths <2.7 Å. Although there is debate as to whether these hydrogen bonds are actually LBHBs,[12–15] these hydrogen bonds are unusual and noteworthy and will be referred to as SSHB.

SSHBs are readily studied in biological macromolecules by high-resolution proton NMR spectroscopy because this method permits their structural assignments. To directly relate structure to function, SSHBs are best studied in enzymes. SSHBs have been proposed as participants in the mechanisms of action of hydrolase enzymes, lyases, a ligase, and several isomerases.[16] NMR spectroscopic evidence for strong hydrogen bonding has been obtained in serine proteases,[17–24] aspartate amino transferase,[25,26] ketosteroid isomerase,[27,28] and triosephosphate isomerase[29] (Fig. 2). It is noteworthy that all SSHBs thus far detected on enzymes involve carboxyl groups.

In this article we show that the proton chemical shift and the fractionation factor of a proton involved in a hydrogen bond are well correlated with the hydrogen bond distances to within ±0.05 Å, increasing the precision to which hydrogen bond distances can be measured in proteins by up to an order of magnitude over that measured by protein X-ray crystallography. The increased precision in these measurements has provided insights toward the overall mechanism and energetic contributions by specific hydrogen bonds to catalysis for several enzymatic reactions.

PROTON CHEMICAL SHIFT

Correlations of hydrogen bond lengths measured by X-ray diffraction with the chemical shift of the proton in the hydrogen bond have established that as hydrogen bonds decrease in length from 3.0 Å to 2.45 Å, that is, proceed from weak to strong (Fig. 1A), the proton becomes more deshielded, that is, its resonance shifts downfield, approaching a maximum value of ≈21 ppm.[30] The reason for the deshielding is the above-mentioned lengthening of the covalent A—H moiety of the A—H···B hydrogen bond as the overall hydrogen bond length decreases. This lengthening attenuates the major shielding provided by the sigma bonding electron pair. Other diamagnetic effects on

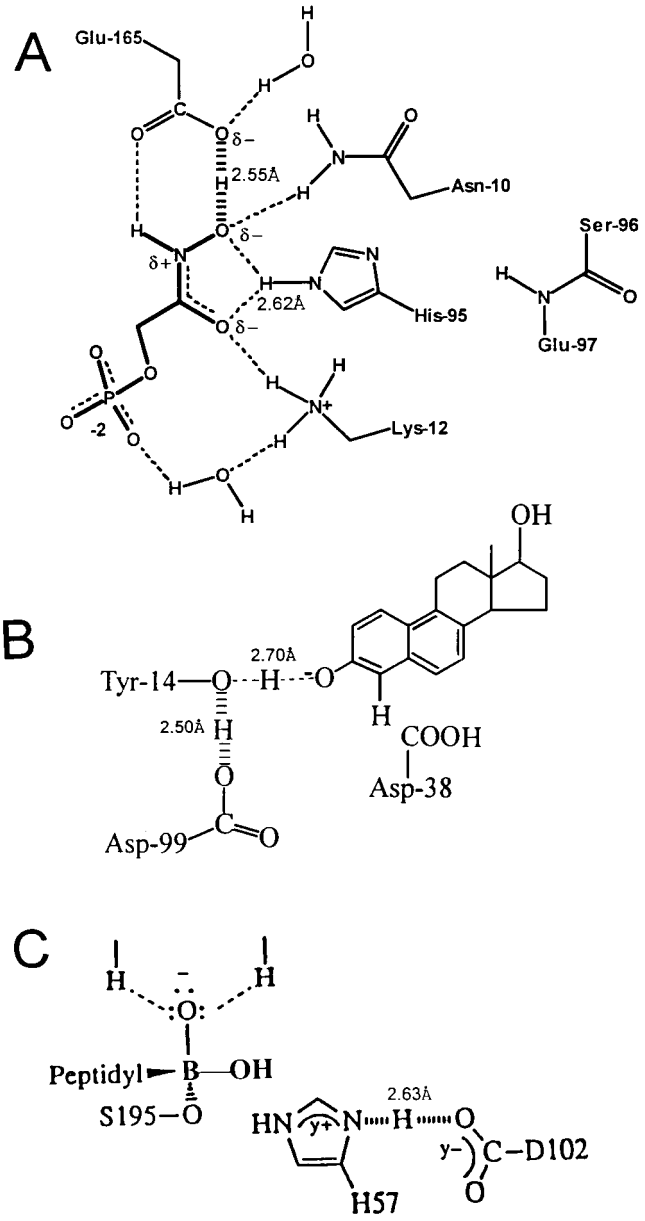

Fig. 2. Examples of SSHBs on enzymes based on NMR data. **(A)** Triosephosphate isomerase complex with phosphoglycolohydroxamic acid (TIM-PGH).[29] **(B)** Ketosteroid isomerase complex of dihydroequilenin (KSI-DHE).[28] **(C)** Chymotrypsin[20] complexed with BoroPhe, forming an analogue of the tetrahedral intermediate.[49]

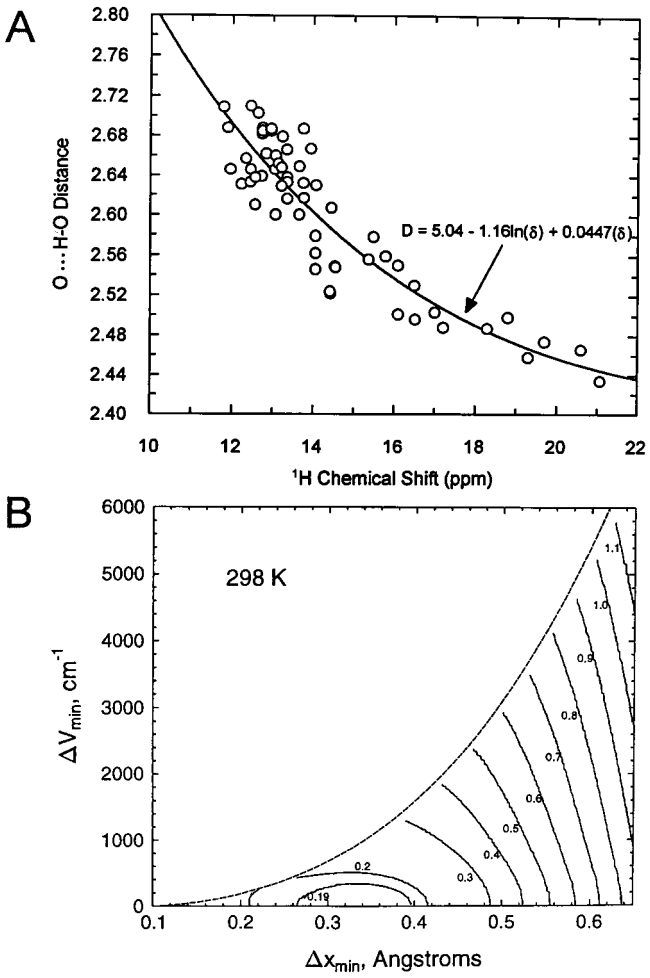

Fig. 3. Graphs for measuring hydrogen bond distances by NMR. **(A)** Correlation of O—H····O hydrogen bond distances (*D*) from X-ray diffraction with ^{1}H chemical shifts (δ) from solid-state NMR of crystalline amino acids. (Data are from McDermott and Ridenour.[30]) **(B)** Estimates of fractionation factors using model one-dimensional, double-minimum quartic potentials according to Kreevoy and Liang.[4] The contours show the dependence of H/D fractionation factors at 25°C on the energy difference between the wells of the double-minimum potential (ΔV_{min}), and the distance between the wells (Δx_{min}).

chemical shifts such as ring currents, secondary structure, and bond anisotropies are at least an order of magnitude smaller.

A rigorous and highly useful correlation of 59 O—H····O hydrogen bond lengths (*D*), measured by small molecule high-resolution X-ray crystallography, with chemical shifts (δ) determined by solid-state NMR in the same crystals[30] is given in Figure 3A. While the data of Figure 3A can be fit by an inverse cubic relationship, which has some theoretical justification for long, weak hydrogen bonds,[31] they are better fit empirically by Equation (2),[28]

$$D = 5.04 - 1.16 \ln(\delta) + 0.0447(\delta) \qquad (2)$$

where *D* refers to the distance between the heavy atoms. The improved fit of the exponential function especially for O—H····O SSHBs may reflect incipient orbital overlap with an exponentially decreasing wave function. Figure 3A and Equation (2) have been very useful in estimating the lengths of O—H····O SSHBs in proteins with errors ≤ 0.05 Å.[28,29] These distances are summarized in Table I and are compared with distances obtained from fractionation factors (see below) and from protein X-ray diffraction. The detection, assignment, and measurement of chemical shifts of resonances of protons that are involved in SSHBs has been described in detail in a methodological review.[2]

TABLE I. Comparison of Hydrogen Bond Lengths on Enzymes Derived From Proton Chemical Shifts (δ) and Fractionation Factors (ϕ) With Those From Protein X-Ray Crystallography

Enzyme complex	Interaction	δ (ppm)	ϕ	Hydrogen bond length (Å) from δ	Hydrogen bond length (Å) from ϕ	Hydrogen bond length (Å) from X-ray	Error range in X-ray[a]
TIM–PGH[b]	E165 · · · HON	14.9[29]	0.38 ± 0.06[29]	2.57 ± 0.05	2.52 ± 0.02	2.68, 3.08[37]	0.19–0.57
	H95 · · · O═C	13.5[29]	0.71 ± 0.02[29]		2.62 ± 0.01	2.66, 3.12[37]	0.19–0.57
KSI–DHE[c]	D99 · · · Y14	18.2[28]	0.34 ± 0.02[28]	2.49 ± 0.02	2.50 ± 0.01	3.9[43]	0.25–0.75
	Y14 · · · $^{-}$O—C	11.6[28]	0.97 ± 0.08[28]	2.72 ± 0.02	2.68 ± 0.02	2.61, 2.63[43]	0.25–0.75
H^+-Chymotrypsinogen	H57 · · · D102	18.1[23]	0.40 ± 0.02[23]		2.54 ± 0.01	2.63, 2.65[48]	0.18–0.54
H^+-Chymotrypsin	H57 · · · D102	18.2[d]	0.64 ± 0.02[d]		2.63 ± 0.01	2.61, 2.65[50]	0.17–0.50
Chymotrypsin-BoroPhe[e]	H57 · · · D102	16.9[d]	0.65 ± 0.01[d]		2.63 ± 0.01	2.70[f]	0.18–0.54
Chymotrypsin-*N*-AcF-CF_3[g]	H57 · · · D102	18.6[24]	0.32 ± 0.01[24]		2.49 ± 0.01	2.63[52]	0.21–0.63
Chymotrypsin-*N*-AcLF-CF_3[h]	H57 · · · D102	18.9[24]	0.43 ± 0.20[24]		2.53 ± 0.08	2.49[52]	0.18–0.54
Subtilisin-BoroPhe[e]	H64 · · · D32	17.4[d]	0.53 ± 0.02[d]		2.60 ± 0.01	2.62[i]	0.20–0.60
Subtilisin-sAAPF[j]	H64 · · · D32					2.62[46]	0.08–0.24

[a]Error range in angstroms is 0.1 to 0.3 times the resolution.
[b]Triosephosphate isomerase complex of phosphoglycolohydroxamic acid.
[c]Ketosteroid isomerase complex of dihydroequilenin.
[d]W. P. Huskey, personal communication. For details, see Bao et al.[49]
[e]BoroPhe is methoxysuccinyl-Ala-Ala-Pro-2-amino-3-phenylethylboronic acid.
[f]Chymotrypsin complex with phenylethane boronic acid.[51]
[g]*N*-AcF-CF_3 is *N*-acetyl-L-phenylalanyltrifluoromethyl ketone.
[h]*N*-AcLF-CF_3 is *N*-acetyl-L-leucyl-L-phenylalanyltrifluoromethyl ketone.
[i]Subtilisin complex with D-*p*-chlorophenyl-1-acetamido boronic acid.[53]
[j]aAAPF is succinyl-alanyl-alanyl-prolyl-phenylalanine.

FRACTIONATION FACTOR

Consider a solvent-exchangeable proton on an enzyme [Eq. (3)].

$$\text{Enz-H} + \text{D}_{\text{solvent}} \rightleftharpoons \text{Enz-D} + \text{H}_{\text{solvent}} \quad (3)$$

The fractionation factor (ϕ) at this position is defined as the equilibrium constant for the exchange of deuterium from the solvent into this position [Eq. (4)].[32]

$$\phi = \frac{[\text{Enz-D}][\text{H}_{\text{solvent}}]}{[\text{Enz-H}][\text{D}_{\text{solvent}}]} \quad (4)$$

Thus ϕ measures the preference of this site for deuterium over protium relative to solvent. If this proton is hydrogen-bonded, the effective force constant of this bond is lower, that is, it vibrates in a wider, shallower well at a lower zero-point frequency or energy (Fig. 1B). The zero-point vibrational frequency or energy of a deuteron at this position, because of its twofold greater mass, is $\leq\sqrt{2}$-fold less sensitive to this decrease in the effective force constant. Hence the zero-point vibrational energy of a deuteron in a hydrogen bond decreases less than that of a proton. As a result, the presence of a deuteron in the hydrogen bond is relatively disfavored over the presence of a proton, yielding a fractionation factor <1 (Fig. 1B). A quantum-mechanical explanation for this equilibrium isotope effect has been given by Kreevoy.[33] The shorter and stronger the hydrogen bond, the lower the fractionation factor, minimizing at a ϕ value of ≈0.16 at an O—H····O hydrogen bond distance of 2.39 Å.[4] At shorter hydrogen bond distances, where a very strong single well hydrogen bond exists, the effective force constant now increases with decreasing distance as the well narrows, increasing the fractionation factor (Fig. 1A).

Using quartic potential functions, Kreevoy and Liang[4] have computed ϕ values of O—H····O hydrogen bonds as a function of distance between the proton wells and these computations have been summarized as a nomograph in Figure 3B (W. P. Huskey, personal communication, 1998), which relates the distance between proton wells to the ϕ values and to the energy difference between the two wells. Figure 3B may be used to determine hydrogen bond lengths from ϕ values by adding two covalent bond lengths, typically 2.00 Å, to the distance between the wells obtained graphically thus assuming linear hydrogen bonds. Bent hydrogen bonds would result in shorter hydrogen bond lengths. As noted above, hydrogen bond strength is essentially independent of hydrogen bond angle over the range 180 ± 30°. Table I compares hydrogen bond distances determined from ϕ values using Figure 3B, with those obtained from chemical shifts using Figure 3A and Equation (2). The agreement is seen to be excellent. Fractionation factors of protons involved in hydrogen bonds are readily measured by NMR by observing the effects on the resonance intensity by variation of the H_2O/D_2O content of the solvent.[27,29,34] By avoiding solvent excitation and using interscan delays well exceeding T_1[2,27–29] systematic errors in the measurement of ϕ due to chemical exchange, solvent viscosity changes, and intramolecular dipolar effects[35] are minimized as shown by good fits to theoretical curves of the relative peak intensities as a function of the mole fraction of H_2O.[27–29] A detailed review of these methods has been published elsewhere.[2]

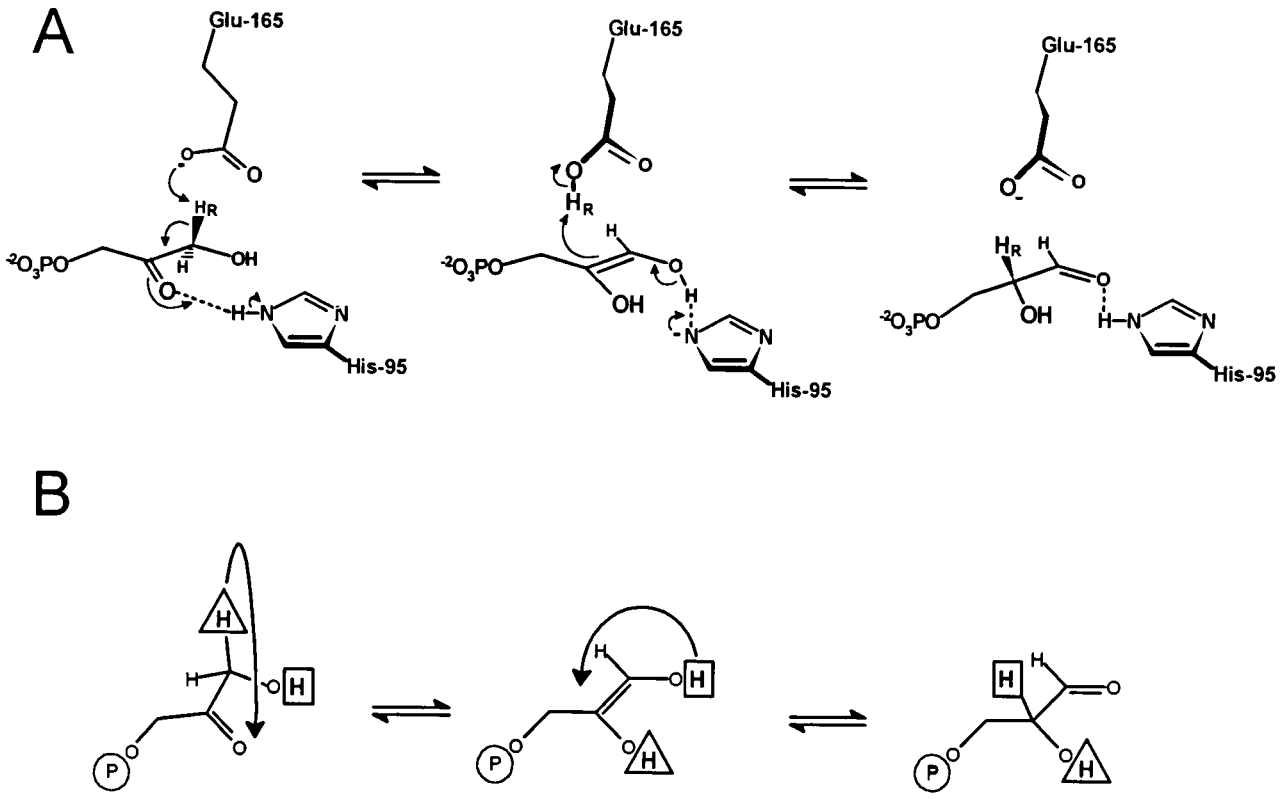

Fig. 4. Mechanisms of triosephosphate isomerase. **(A)** Classical mechanism.[39,54] **(B)** Proton transfers in the criss-cross-mechanism mediated by Glu-165.[29,38,39]

Other NMR methods for measuring hydrogen bond lengths are less precise, including the recently described heteronuclear method for measuring the quadrupolar coupling constant of D in N—D····O hydrogen bonds from longitudinal deuteron relaxation rates.[36] This method, calibrated by imprecise protein crystallography, requires both ^{13}C and ^{15}N labeling, as well as the spectral density function, correlation time, and order parameter for each N—D vector, necessitating additional ^{15}N relaxation measurements.

TRIOSEPHOSPHATE ISOMERASE

TIM catalyzes the reversible tautomerization of DHAP and GAP, with Glu-165 removing the pro-R proton from C1 of DHAP and neutral His-95 polarizing the carbonyl group of the substrate (Fig. 4A). Figure 2A shows the structure of the TIM active site with bound PGH, an analogue of the enediolic intermediate, based on X-ray[37] and NMR studies.[29] A strong hydrogen bond was detected between the 1-NOH proton of PGH and a carboxyl oxygen of the general base catalyst, Glu-165, on the basis of the ≈6.2 ppm downfield shift of the 1-NOH proton resonance and its low fractionation factor, $\phi = 0.38$. Although the strength of this hydrogen bond is difficult to measure, its length is short. From the correlation of OH····O hydrogen bond distances with chemical shifts (Fig. 3A), using Equation (2), the chemical shift of 14.9 ppm for the 1-NOH resonance corresponds to a distance of 2.57 ± 0.05 Å for the PGH NOH····Glu-165 hydrogen bond (Table I). An independent measurement of this hydrogen bond length of 2.52 ± 0.02 Å is obtained from the measured fractionation factor $\phi = 0.38 \pm 0.06$ using Figure 3B. These distances, based on two independent NMR measurements, show good agreement. They also overlap with the shorter of the two PGH NOH····Glu-165 hydrogen bond distances in the two subunits of the crystalline, homodimeric TIM–PGH complex obtained by X-ray diffraction, 2.68 ± 0.19 Å. The minimum error in the X-ray determined distance of 0.1 times the resolution is assumed.

The His-95 NεH proton forms a moderately strong hydrogen bond with the 2-carbonyl oxygen of PGH (Fig. 2A) with a chemical shift of 13.5 ppm (0.4 ppm downfield from its position in the free enzyme) and a fractionation factor of 0.71 ± 0.02.[29] Because this is a NH····O hydrogen bond, its distance was not calculated from the correlation in Figure 3A , which is for OH····O hydrogen bonds. However, using Figure 3B and $\phi = 0.71 \pm 0.02$, a PGH C═;O····His-95 hydrogen bond distance of 2.62 ± 0.01 Å was obtained , which is in good agreement with the shorter of the two distances given by the X-ray structure (Table I).

While the hydrogen bond from His-95 NεH to the 2-carbonyl oxygen of PGH (Fig. 2A) likely promotes carbonyl polarization, thereby facilitating catalysis (Fig. 4A), the role of the SSHB between the carboxyl group of

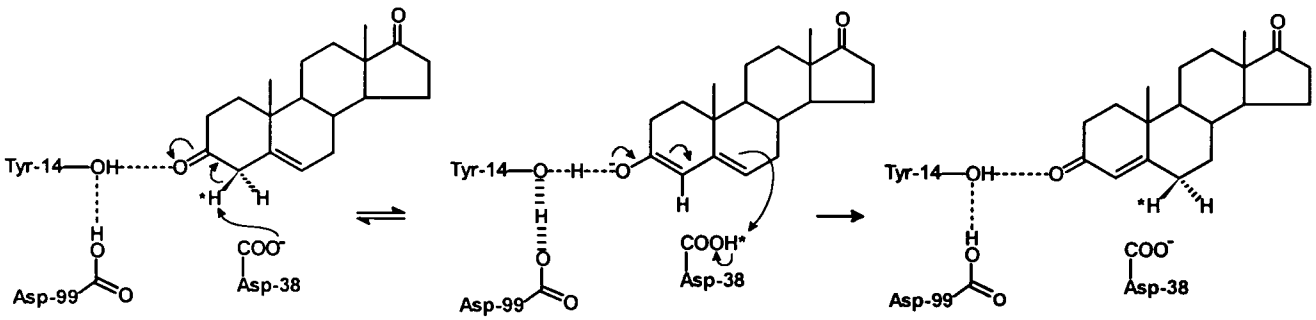

Fig. 5. Catalytic diad mechanism of ketosteroid isomerase utilizing a short, strong hydrogen bond between the protonated form of Asp-99 and Tyr-14.[28,40]

Glu-165 and the O1 oxygen of PGH is not clear. In the H95Q mutant, it may participate in proton transfer from O1 to C2 of the enediol intermediate as part of a crisscross mechanism (Fig. 4B).[29,38] In wild-type TIM the crisscross mechanism of proton transfer may not contribute greatly to catalysis because it predicts that the observed conservation of ≈2% tritium from the C1 of the substrate DHAP to C2 of the product GAP be intermolecular. Experimentally, this conservation of tritium has been shown to be entirely intramolecular consistent with the mechanism of Figure 4A.[39] Alternatively, the SSHB between PGH-NOH and Glu-165 may be the fortuitous result of a close match of the pK_a values of Glu-165 and the NOH of PGH, which does not occur in the enediol.[1]

KETOSTEROID ISOMERASE

KSI catalyzes the conversion of Δ^5- to Δ^4-3-ketosteroids via a dienolic intermediate, with Asp-38 removing the axial proton from the C4 position of the steroid, concerted with polarization of the 3-keto group by both Tyr-14 and the protonated carboxyl group of Asp-99 (Fig. 5). Figure 2B shows the solution structure of the complex of KSI with DHE based on distance constraints obtained from NMR studies of highly deshielded protons at the active site of isomerase.[28] The hydrogen bond length from Asp-99—COOH to Tyr-14—OH, obtained from the chemical shift of 18.15 ppm for the carboxyl proton, is 2.49 ± 0.02 Å using Figure 3A and Equation (2) (Table I). The fractionation factor of 0.34 ± 0.02 yields an independent measurement of 2.50 ± 0.01 Å using Figure 3B consistent with a SSHB. The hydrogen bond length from Tyr-14—OH to the steroid oxygen, obtained from its chemical shift of 11.6 ppm is 2.72 ± 0.02 Å, and independently obtained from its fractionation factor of 0.97 ± 0.08 is 2.68 ± 0.02 Å indicating a normal hydrogen bond. The solution structure of KSI complexed with 19-nortestosterone hemisuccinate, a product analogue and substrate in the reverse isomerase reaction, is compatible with these measured distances and with a hydrogen-bonded catalytic diad, Asp-99—COOH····Tyr-14—OH····O—steroid , which acts as the acid catalyst.[40] In this mechanism, a normal hydrogen bond between Asp-99 and Tyr-14 in the substrate complex increases in strength to form a LBHB as the intermediate dienolate forms (Fig. 5). This strengthening effect is transmitted to the Tyr-14—OH····O-steroid in the transition state, facilitating polarization of the 3-keto group.[28,40] Making use of active site mutants, the strength of this hydrogen bond has been estimated by three independent approaches to be ≤ −7 kcal/mol.[27,41,42]

The 2.5-Å resolution X-ray structure of a homologous KSI complexed with DHE[43] yields hydrogen bond lengths between the Tyr-14—OH and the steroid oxygen of 2.61 and 2.63 Å, in the two subunits, in agreement with those determined by NMR. A much greater distance of 3.9 Å is found between Asp-99—COOH and Tyr-14—OH. It is noted that the errors in such distances from protein X-ray crystallography can be as great as ±0.75 Å, that is, 0.3 times the resolution (2.5 Å). The distance of 3.9 Å has been interpreted in terms of the separate donation to the steroid oxygen of normal hydrogen bonds by both Tyr-14 and Asp-99. This alternative mechanism of acid catalysis is inconsistent with the effects of mutations on catalysis and on the low field NMR spectra. The double mutation of the general base, Asp-38 to Asn, and of Tyr-14 to Phe completely abolishes all enzymatic activity despite the presence of Asp-99.[44] The single mutation of Tyr-14 to Phe abolishes the resonances of both Asp-99—COOH (at 18.15 ppm) and Tyr-14—OH (at 11.6 ppm).[27,45] Ab initio quantum-mechanical calculations reveal that the intermediates predicted by both mechanisms are isoenergetic only when both intermediates have a SSHB, emphasizing the importance of strong hydrogen bonding in this system (M. A. McAllister, personal communication, 1998).

SERINE PROTEASES

Serine proteases share a common active site composed of an oxyanion hole and a catalytic triad consisting of a Ser, a His, and an Asp (Fig. 2C). The Nϵ nitrogen of His functions first as a general base catalyst, deprotonating Ser for nucleophilic attack at the substrate carbonyl group, which is polarized by the oxyanion hole, resulting in formation of the tetrahedral intermediate. Then His NϵH functions as a general acid catalyst for protonating the departing amine. The resulting acyl–enzyme intermediate is then hydrolyzed by a water molecule to regenerate the enzyme for the next catalytic cycle.

Table I lists six determinations by NMR of hydrogen bond lengths between the Asp and His residues of the

catalytic triad under conditions that resemble formation of the tetrahedral intermediate, that is, the catalytic His is protonated. In each case, NMR spectra showed a downfield proton chemical shift and low fractionation factor for the Nδ H proton of the catalytic His , which is hydrogen-bonded to the catalytic Asp. Hydrogen bond lengths for the Asp····His interaction as calculated from the measured fractionation factors, using Figure 3B, range from 2.49 to 2.63 Å, which are much less than the van der Waals contact distance of 2.9 Å between nitrogen and oxygen, indicating SSHB formation in the mechanism of serine proteases. These distances are in good agreement with those measured by protein X-ray crystallography, although the errors in the latter are much greater (Table I). An unusually precise distance of 2.62 ± 0.08 Å has recently been determined by protein X-ray crystallography at 0.78 Å resolution for the Asp····His interaction in the product complex of subtilisin with sAAPF at pH 5.9.[46] This ultrahigh-resolution structure provides increased definition, visualizing hydrogen atoms, and confirms a SSHB to His in the catalytic triad.

According to the conventional general base mechanism, the Asp carboxyl group is hydrogen-bonded to the His Nδ H and is thought to correctly orient the His Nϵ nitrogen to activate Ser for nucleophilic attack. The Asp····His hydrogen bond distance is apparently compressed upon binding the petidyl group, promoting LBHB formation, which serves to increase the basicity of the His Nϵ nitrogen (Fig. 6). Increased basicity for His Nϵ would enhance its reactivity in abstracting the proton from Ser and thereby lower the activation barrier for formation of the tetrahedral intermediate.[20] The strength of this hydrogen bond has been estimated to be −7 kcal/mol from the ΔpK_a of 5.2 log units for the catalytic His in trifluoromethyl ketone complexes of chymotrypsin in comparison with that of the model dipeptide Asp–His.[20] The value of −7 kcal/mol is consistent with the effects of mutations of the Asp–His diad of serine proteases, which decrease catalysis by factors of 10^4- to 10^6-fold.[19,47]

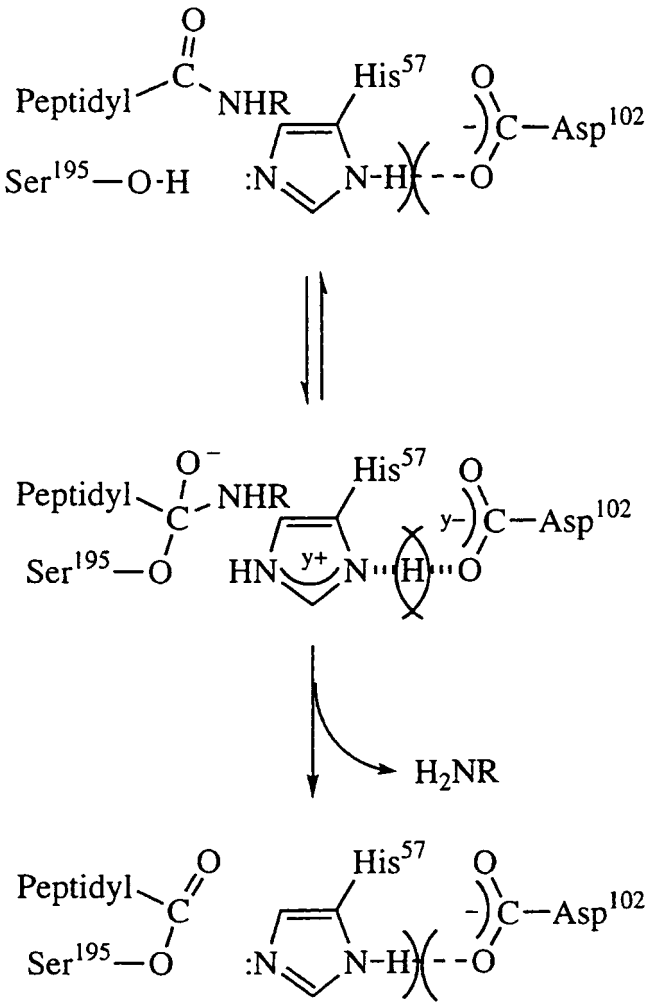

Fig. 6. Mechanism of acylation of chymotrypsin utilizing a short, strong hydrogen bond between Asp-102 and the protonated form of His-57.[20]

ACKNOWLEDGMENTS

We thank W. Phillip Huskey for permission to reproduce Figure 3B and data in Table I before publication, and for helpful discussions, and Ann E. McDermott for permission to reproduce Figure 3A.

REFERENCES

1. Cleland WW, Frey PA, Gerlt JA. The low barrier hydrogen bond in enzymatic catalysis. J Biol Chem 1998;273:25529–25532.
2. Mildvan AS, Harris TK, Abeygunawardana C. NMR methods for the detection and study of low-barrier hydrogen bonds on enzymes. Methods Enzymol 1999;308; in press.
3. Hibbert F, Emsley J. Hydrogen bonding and chemical reactivity. Advances in Physical Organic Chem 1990;26:255–379.
4. Kreevoy MM, Liang TM. Structures and isotopic fractionation factors of complexes, $A_1HA_2^{-1}$. J Am Chem Soc 1980;102:3315–3322.
5. Steiner Th, Saenger W. Lengthening of the covalent O—H bond in O—H····O hydrogen bonds re-examined from low-temperature neutron diffraction data of organic compounds. Acta Crystallogr 1994;B50:348–357.
6. Donohue J. Structural chemistry and molecular biology. San Francisco: WH Freeman, 1968. p 443.
7. Adalsteinsson H, Maulitz AH, Bruice TC. Calculation of the potential energy surface for intermolecular amide hydrogen bonds using semiempirical and ab initio methods. J Am Chem Soc 1996;119:7689–7693.
8. Smallwood CJ, McAllister MA. Characterization of low-barrier hydrogen bonds. 7. Relationship between strength and geometry of short-strong hydrogen bonds. The formic acid–formate anion model system. An ab initio and DFT investigation. J Am Chem Soc 1997;119:11277–11281.
9. Shan S, Herschlag D. The change in hydrogen bond strength accompanying charge rearrangement: implications for enzymatic catalysis. Proc Natl Acad Sci USA 1996;93:14474–14479.
10. Makhatadze GI, Privalov P. Energetics of protein structure. Adv Protein Chem 1995;47:307–425.
11. Watson JD, Hopkins NH, Roberts JW, Steitz JA, Weiner AM. Molecular biology of the gene. Menlo Park, CA: Benjamin/Cummings, 1987. p 132–138.
12. Warshel A, Papazyan A, Kollman PA. On low-barrier hydrogen bonds and enzyme catalysis. Science 1995;269:102–104.
13. Warshel A., Papazyan A. Energy considerations show that low-barrier hydrogen bonds do not offer a catalytic advantage over ordinary hydrogen bonds. Proc Natl Acad Sci USA 1996;93:13665–13670.
14. Guthrie JP. Short strong hydrogen bonds: can they explain enzymic catalysis? Chem Biol 1996;3:163–170.

15. Scheiner S, Kar T. The nonexistence of specially stabilized hydrogen bonds in enzymes. J Am Chem Soc 1995;117:6970–6975.
16. Cleland WW, Kreevoy MM. Low-barrier hydrogen bonds and enzymatic catalysis. Science 1994;264:1887–1890.
17. Robillard G, Shulman RG. High-resolution nuclear magnetic resonance studies of the active site of chymotrypsin. I. The hydrogen bonded protons of the "charge relay" system. J Mol Biol 1972;71:519–540.
18. Golubev NS, Gindin VA, Ligai SS, Smirnov SN. Study of hydrogen bonds in the catalytic triad of trypsin using ^{1}H, ^{13}C, and ^{15}N NMR spectra. Biochemistry (Moscow) 1994;59:613–624.
19. Frey PA, Whitt SA, Tobin JB. A low-barrier hydrogen bond in the catalytic triad of serine proteases. Science 1994;264:1927–1930.
20. Cassidy CS, Lin J, Frey PA. A new concept for the mechanism of action of chymotrypsin: the role of the low-barrier hydrogen bond. Biochemistry 1997;36:4576–4584.
21. Markley J, Ibanez IB. Zymogen activation in serine proteases: proton magnetic resonance pH titration studies of the two histidines of bovine chymotrypsinogen A and α-chymotrypsin. Biochemistry 1978;17:4637–4640.
22. Liang T-C, Abeles RH. Complex of α-chymotrypsin and N-acetyl-L-leucyl-L-phenylalanyltrifluoromethyl ketone: structural studies with NMR spectroscopy. Biochemistry 1987;26:7603–7608.
23. Markley JL, Westler WM. Protonation-state dependence of hydrogen bond strengths and exchange rates in a serine protease catalytic triad: bovine chymotrypsinogen A. Biochemistry 1996;35: 11092–11097.
24. Lin J, Westler WM, Cleland WW, Markley JL, Frey PA. Fractionation factors and activation energies for exchange of the low barrier hydrogen bonding proton in peptidyl trifluoromethyl ketone complexes of chymotrypsin. Proc Natl Acad Sci USA 1998;95: 14664–14668.
25. Kintanar A, Metzler CM, Metzler DE, Scott RD. NMR observation of exchangeable protons of pyridoxal phosphate and histidine residues in cytosolic aspartate aminotransferase. J Biol Chem 1991;266:17222–17229.
26. Mollova E, Metzler DE, Kintanar A, Kagamiyama H, Hayashi H, Hirotsu K, Miyahara I. Use of ^{1}H–^{15}N heteronuclear multiple-quantum coherence NMR spectroscopy to study the active site of aspartate aminotransferase. Biochemistry 1997;36:615–625.
27. Zhao Q, Abeygunawardana C, Talalay P, Mildvan AS. NMR evidence for the participation of a low-barrier hydrogen bond in the mechanism of Δ^5-3-ketosteroid isomerase. Proc Natl Acad Sci USA 1996;93:8220–8224.
28. Zhao Q, Abeygunawardana C, Gittis AG, Mildvan AS. Hydrogen bonding at the active site of Δ^5-3-ketosteroid isomerase. Biochemistry 1997;36:14616–14626.
29. Harris TK, Abeygunawardana C, Mildvan AS. NMR studies of the role of hydrogen bonding in the mechanism of triosephosphate isomerase. Biochemistry 1997;36:14661–14675.
30. McDermott A, Ridenour CF. Proton chemical shift measurements in biological solids. In: Encyclopedia of NMR. Sussex, UK: Wiley, 1996:3820–3825.
31. Wagner G, Pardi A, Wüthrich K. Hydrogen bond length and ^{1}H NMR chemical shifts in proteins. J Am Chem Soc 1983;105:5948–5949.
32. Schowen KB, Schowen RL. Solvent isotope effects on enzyme systems. Methods Enzymol 1982;87:551–606.
33. Kreevoy MM. The exposition of isotope effects on rates and equilibria. J Chem Educ 1964;41:636–638.
34. Loh SN, Markley JL. Hydrogen bonding in proteins as studied by amide hydrogen D/H fractionation factors: application to staphylococcal nuclease. Biochemistry 1994;33:1029–1036.
35. LiWang AC, Bax A. Equilibrium protium/deuterium fractionation of backbone amides in U–^{13}C/^{15}N labeled human ubiquitin by triple resonance NMR. J Am Chem Soc 1996;118:12864–12865.
36. LiWang AC, Bax A. Solution NMR characterization of hydrogen bonds in a protein by indirect measurement of deuterium quadrupole couplings. J Magn Reson 1997;127:54–64.
37. Davenport RC, Bash PA, Seaton BA, Karplus M, Petsko GA, Ringe D. Structure of the triosephosphate isomerase–phosphoglycolohydroxamate complex: an analogue of the intermediate on the reaction pathway. Biochemistry 1991;30:5821–5826.
38. Nickbarg EB, Davenport RC, Petsko GA, Knowles JR. Triosephosphate isomerase: removal of a putatively electrophilic histidine residue results in a subtle change in catalytic mechanism. Biochemistry 1988;27:5948–5960.
39. Harris TK, Cole RN, Comer FI, Mildvan AS. Proton transfer in the mechanism of triosephosphate isomerase. Biochemistry 1998;37: 16828–16838.
40. Massiah MA, Abeygunawardana C, Gittis AG, Mildvan AS. Solution structure of Δ^5-3-ketosteroid isomerase complexed with the steroid 19-nortestosterone hemisuccinate Biochemistry 1998;37: 14701–14712.
41. Kuliopolus A, Mildvan AS, Shortle D, Talalay P. Kinetic and ultraviolet spectroscopic studies of active-site mutants of Δ^5-3-ketosteroid isomerase. Biochemistry 1989;28:149–159.
42. Xue L, Talalay P, Mildvan AS. Studies of the catalytic mechanism of an active-site mutant (Y14F) of Δ^5-3-ketosteroid isomerase by kinetic deuterium isotope effects. Biochemistry 1991;30:10858–10865.
43. Kim SW, Cha S-S, Cho H-S, Kim J-S, Ha N-C, Cho M-J, Joo S, Kim KK, Choi KY, Oh B-H. High-resolution crystal structures of Δ^5-3-ketosteroid isomerase with and without a reaction intermediate analogue. Biochemistry 1997;36:14030–14036.
44. Kuliopulos A, Talalay P, Mildvan AS. Combined effects of two mutations of catalytic residues on the Δ^5-3-ketosteroid isomerase reaction. Biochemistry 1990;29:10271–10280.
45. Zhao Q, Abeygunawardana C, Mildvan AS. NMR studies of the secondary structure in solution and the steroid binding site of Δ^5-3-ketosteroid isomerase in complexes with diamagnetic and paramagnetic steroids. Biochemistry 1997;36:3458–3472.
46. Kuhn P, Knapp M, Soltis SM, Granshaw G, Thoene M, Bott R. The 0.78 Å structure of a serine protease: *Bacillus lentus* subtilisin. Biochemistry 1998;37:13446–13452.
47. Carter P, Wells J. Dissecting the catalytic triad of a serine protease. Nature 1988;332:564–568.
48. Wang D, Bode W, Huber R J. Bovine chymotrypsinogen A X-ray crystal structure analysis and refinement of a new crystal form at 1.8-Å resolution. J Mol Biol 1985;185:595–624.
49. Bao D, Kettner C, Huskey WP, Jordan F. Distinguished hydrogen bonding to active-site histidine in peptidyl boronic acid inhibitor complexes of chymotrypsin and subtilisin: proton magnetic resonance assignments and H/D fractionation. J Am Chem Soc 1999; in press.
50. Tsukada H, Blow DM. Structure of α-chymotrypsin refined at 1.68-Å resolution. J Mol Biol 1985;184:703–711.
51. Tulinsky A, Blevins RA. Structure of a tetrahedral transition state complex of α-chymotrypsin dimer at 1.8-Å resolution. J Biol Chem 1987;262:7737–7743.
52. Brady K, Wei A, Ringe D, Abeles RH. Structure of chymotrypsin–trifluoromethyl ketone inhibitor complexes: comparison of slowly and rapidly equilibrating inhibitors. Biochemistry 1990;29:7600–7607.
53. Stoll VS, Eger BT, Hynes RC, Martichonok V, Jones JB, Pai EF. Differences in binding modes of enantiomers of 1-acetamido boronic acid based protease inhibitors: crystal structures of γ-chymotrypsin and subtilisin carlsberg complexes. Biochemistry 1998; 37:451–462.
54. Nickbarg EB, Knowles JR. Triosephosphate isomerase: energetics of the reaction catalyzed by the yeast enzyme expressed in *Escherichia coli*. 1988;Biochemistry 27:5939–5947.